

# Seismic Constraints on the Nature of Lower Crustal Reflectors Beneath the Extending Southern Transition Zone of the Colorado Plateau, Arizona

TOM PARSONS, JOHN M. HOWIE, AND GEORGE A. THOMPSON

*Department of Geophysics, Stanford University, Stanford, California*

We determine the reflection polarity and exploit variations in  $P$  and  $S$  wave reflectivity and  $P$  wave amplitude versus offset (AVO) to constrain the origin of lower crustal reflectivity observed on new three-component seismic data recorded across the structural transition of the Colorado Plateau. The near vertical incidence reflection data were collected by Stanford University in 1989 as part of the U.S. Geological Survey Pacific to Arizona Crustal Experiment that traversed the Arizona Transition Zone of the Colorado Plateau. The results of independent waveform modeling methods are consistent with much of the lower crustal reflectivity resulting from thin, high-impedance layers. The reflection polarity of the cleanest lower crustal events is positive, which implies that these reflections result from high-velocity contrasts, and the waveform character indicates that the reflectors are probably layers less than or approximately equal to 200 m thick. The lower crustal events are generally less reflective to incident  $S$  waves than to  $P$  waves, which agrees with the predicted behavior of high-velocity mafic layering. Analysis of the  $P$  wave AVO character of lower crustal reflections demonstrates that the events maintain a constant amplitude with offset, which is most consistent with a mafic-layering model. One exception is a high-amplitude (10 dB above background) event near the base of lower crustal reflectivity which abruptly decreases in amplitude at increasing offsets. The event has a pronounced  $S$  wave response, which along with its negative AVO trend is a possible indication of the presence of fluids in the lower crust. The Arizona Transition Zone is an active but weakly extended province, which causes us to discard models of lower crustal layering resulting from shearing because of the high degree of strain required to create such layers. Instead, we favor horizontal basaltic intrusions as the primary origin of high-impedance reflectors based on (1) The fact that most xenoliths in eruptive basalts of the Transition Zone are of mafic igneous composition, (2) indications that a pulse of magmatic activity crossed the Transition Zone in the late Tertiary period, and (3) the high regional heat flow observed in the Transition Zone. The apparent presence of fluids near the base of the reflective zone may indicate a partially molten intrusion. We present a mechanism by which magma can be trapped and be induced to intrude horizontally at rheologic contrasts in extending crust.

## INTRODUCTION

Laminated reflectivity in the lower crust is commonly observed on deep crustal seismic sections recorded in tectonically extended terranes [Clowes *et al.*, 1968; Fuchs, 1969; BIRPS and ECORS, 1986; Potter *et al.*, 1987; McCarthy and Thompson, 1988; Klemperer, 1989]. Possible causes of laminated reflectivity include compositional layering [e.g., Christensen, 1989; Green *et al.*, 1990], low-velocity, fluid-filled shear zones [e.g., O'Connell and Budiansky, 1974; Meissner and Kuszniir, 1987], and horizontal magmatic intrusions [e.g., Meissner and Wever, 1986; Warner, 1990]. Such reflectivity can be successfully reproduced on synthetic sections based on any of the above models, and discontinuous reflectivity can be reproduced from random-scattering models [Levander and Gibson, 1991]. In this paper we estimate the polarity of lower crustal events on near-vertical incidence seismic data recorded in the Transition Zone of the southern Colorado Plateau in Arizona, U.S.A., and correlate the results with independent analyses of  $P$  and  $S$  wave reflectivity and  $P$  wave amplitude versus offset.

The Transition Zone marks the most recent encroachment of Basin and Range Province extension into the Colorado Plateau and is a zone of tectonic gradation from the highly

extended metamorphic core complexes of the southern Basin and Range Province to the nonextended Colorado Plateau. Seismicity associated with normal faulting [Eberhart-Phillips *et al.*, 1981] and high surface heat flow [Lachenbruch and Sass, 1978; J. H. Sass *et al.*, manuscript in preparation, 1992] indicate that extension is ongoing. Initially horizontal diabase sheet intrusions of middle Proterozoic age have been tilted in places and outcrop at various localities across the Arizona Transition Zone and are thought to have been intruded from shallow depths down to levels as deep as 13 km [Howard, 1991]. Diabase sheets are the cause of the Bagdad reflection sequence, a package of widespread, high-amplitude reflections first observed on industry reflection profiles from the Transition Zone [Galvan and Frost, 1985] and on the Consortium for Continental Reflection Profiling (COCORP) Arizona reflection sections [Hauser *et al.*, 1987]. The presence of layering in the upper crust of known velocity and thickness allows us to apply important constraints on waveform analysis of deeper events of unknown origin.

The near-vertical incidence data were collected by Stanford University as part of the 1989 Pacific to Arizona Crustal Experiment (PACE), organized by the U.S. Geological Survey (USGS) and university affiliates. The Stanford recording array was situated across Chino Valley at the physiographic boundary between the Colorado Plateau and the Transition Zone (Figure 1) and recorded 22 large (450–3600 kg) chemical explosions of the USGS wide-angle array. The Stanford array emphasized three-component  $P$  and  $S$

Copyright 1992 by the American Geophysical Union.

Paper number 92JB00947.  
0148-0227/92/92JB-00947\$05.00

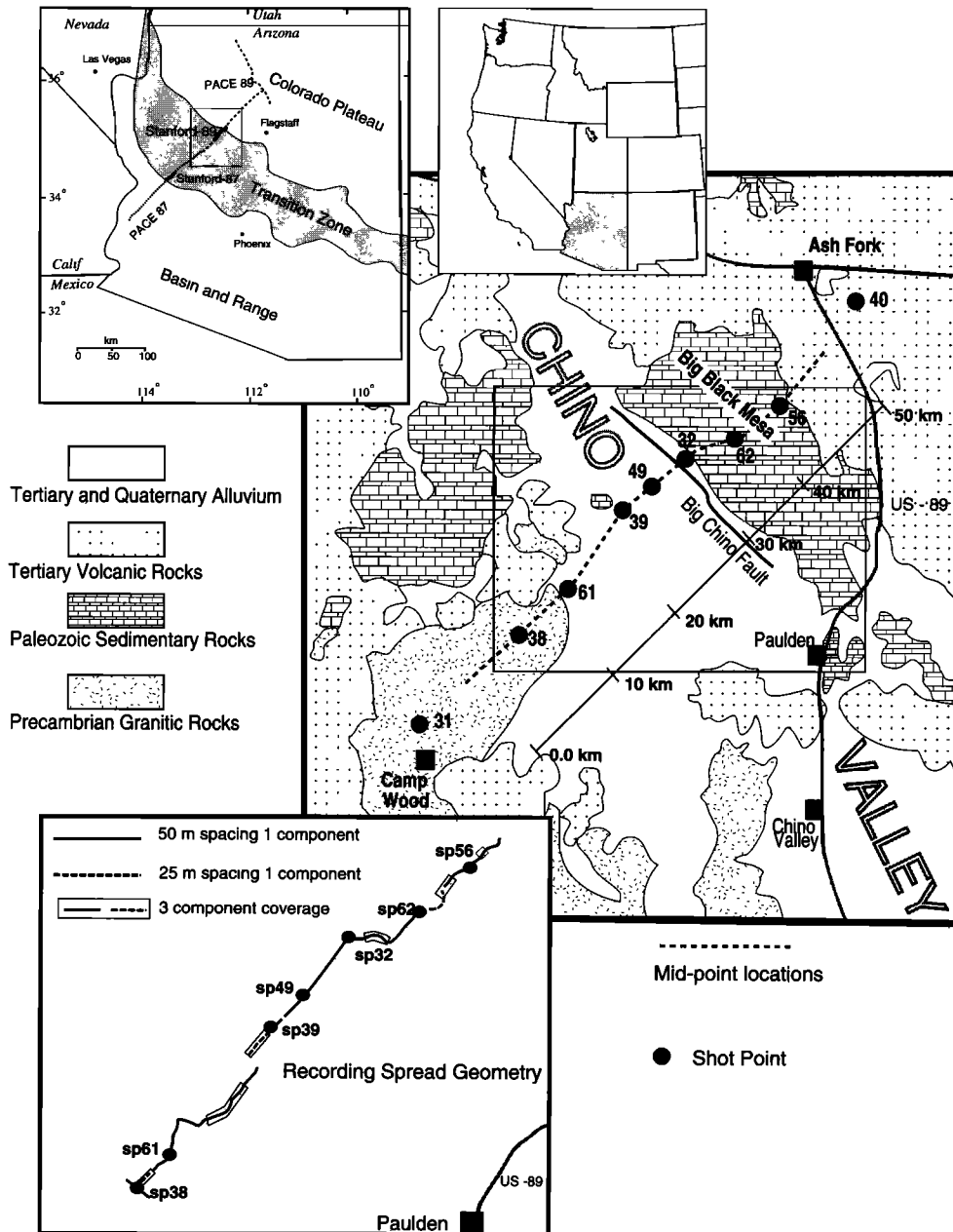


Fig. 1. Geologic map showing the Stanford Colorado Plateau reflection experiment located at the northwestern edge of the Transition Zone between the extended Basin and Range Province and the nonextended Colorado Plateau. The dotted line on the geologic map shows the approximate midpoint locations of the in line shots. The top left inset map shows the position of the Stanford profile relative to the USGS Pacific to Arizona Crustal Experiment (PACE) and tectonic provinces, and the lower inset shows the actual recording geometry used for the Stanford profile.

wave recording and tight (25–50 m) station spacing. The spread was 45 km long and consisted of 1700 channels recorded on two industry reflection systems. The reflection sections show a laminated reflective lower crust, a transitional Moho (Figure 2), and a relatively transparent upper crust with isolated subcontinuous high-amplitude events which are part of the Bagdad reflection sequence [Howie *et al.*, 1991] (Figure 3). The lower crustal reflectivity begins at about 6 s two-way travel time (twtt), and the highest-amplitude lower crustal reflectivity is outlined above and below in time by continuous events at about 7 and 9 s twtt. In this paper we consider continuous reflections as horizons

that are traceable for 10 to 20 km but can be interrupted by interference and defocusing effects and may be composed of individual segments from 1 to 5 km in length.

One way to resolve in part the origin of laminated lower crustal reflectivity is to determine the reflection polarity of the events. For example, knowledge of the reflection polarity can help distinguish between low-impedance layers like shear zones or partial melts and high-impedance mafic layers, which will have opposite polarities. However, polarity determination of reflections from a deeply penetrating seismic signal is difficult because the signal is heavily filtered by the Earth, and the frequency bandwidth is typically

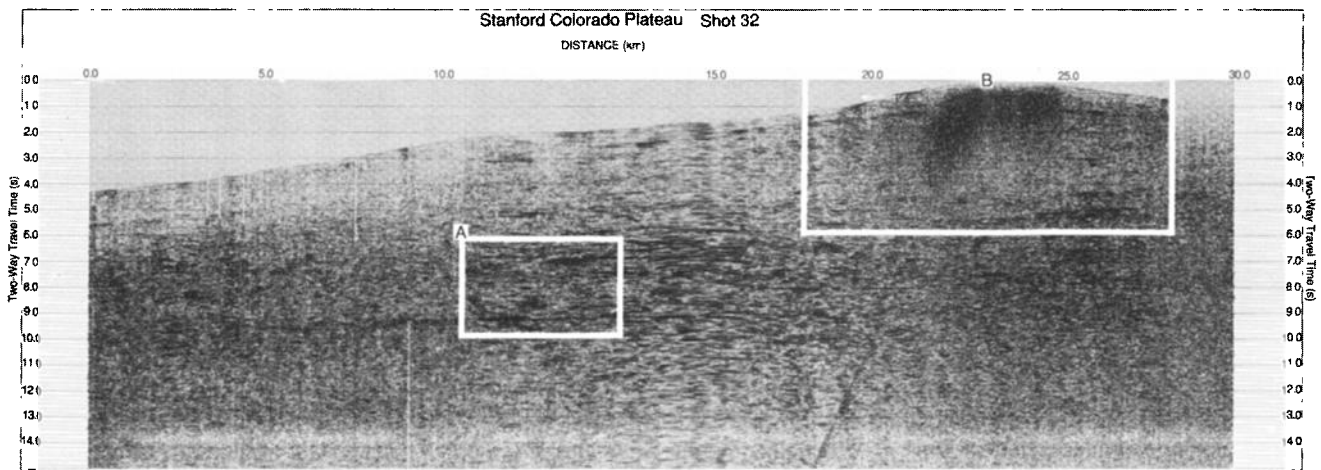


Fig. 2. Shot gather from shot 32 (2800 kg) showing the reflective character of the vertical incidence data. The reflective lower crust begins at about 6 s two-way travel time (twtt) and decreases gradually until about 12–13 s twtt at the Moho. Window (A) is the zone investigated for reflection polarity, *P* and *S* wave reflectivity, and *P* wave amplitude versus offset. The upper crust is seismically transparent with the exception of some events from the Bagdad reflection sequence (window B is shown in close-up in Figure 3). The crust is about 39 km thick at the edge of the Colorado Plateau, and the Moho is picked at the depth where reflectivity dies out. The data were corrected for spherical divergence and normal move-out and were band-pass filtered. The location of the shot point is at kilometer 23.

reduced to a small fraction of the initial source bandwidth. The observed vertical incidence seismogram  $x(t)$  may be thought of as a series of convolutions

$$x(t) = s(t) * e_d(t) * r(t) * e_u(t) * a(t),$$

where  $s(t)$  is the seismic source,  $e_d(t)$  and  $e_u(t)$  represent filtering by the Earth for the downgoing and upgoing paths,  $r(t)$  is the reflector response,  $a(t)$  is the response of the recording array, and  $t$  is time. The goal of polarity determi-

nation is to isolate the reflector response  $r(t)$  from the observed seismogram  $x(t)$ , which requires accurate estimation of the source wavelet. If the signal-to-noise ratio of the reflection data is high, and if surface conditions are relatively homogeneous, the direct arrival is a good approximation of the source waveform [Hill, 1974] and may be used to model reflection polarity [e.g., Goodwin et al., 1989; Meissner et al., 1984].

In this study we use the direct arrival from a 2800-kg

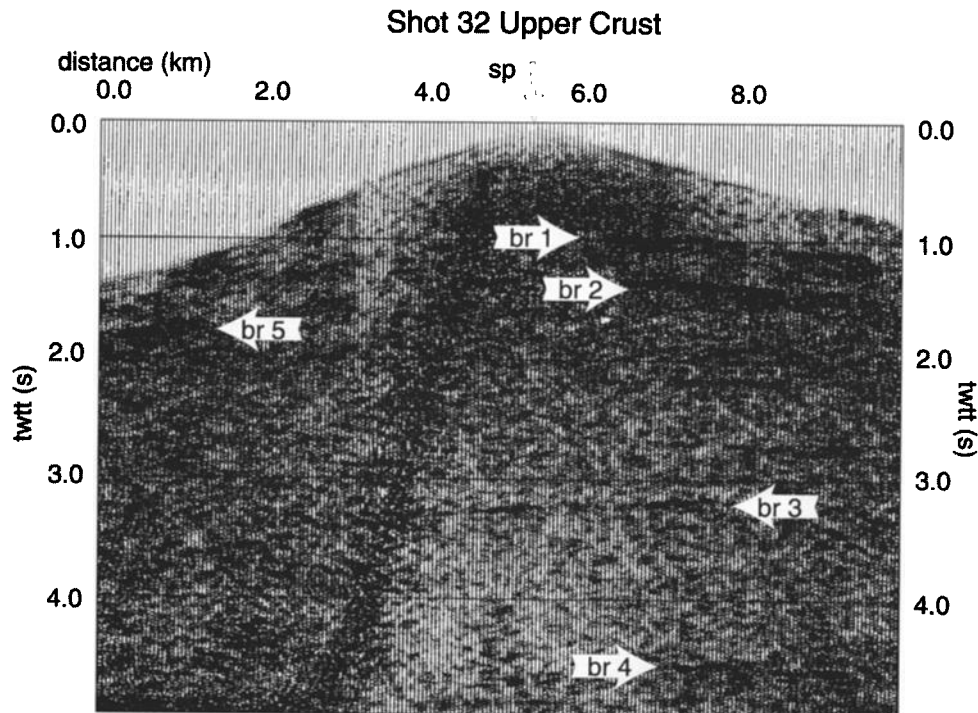


Fig. 3. Close-up window of the upper crust (shot 32) showing events of the Bagdad reflection sequence. The reflection at 1 s two-way travel time (twtt) (br 1) is stacked and deconvolved in Figure 5c and is used to correlate the source wavelet.

explosive source (shot 32 in Figure 1), detonated and recorded on crystalline granitic rocks, to estimate the seismic source character  $s(t)$ . By calibrating with a reflection from a known velocity contrast, we can determine if the direct arrival is a good approximation of the source, as well as determine if the recording array  $a(t)$  has had an effect on the phase of the waveform. Since the Bagdad reflections are known to have positive polarity [Goodwin *et al.*, 1989; Litak *et al.*, 1991], we utilize these reflections as a benchmark to assure that the direct arrival employed is a valid representation of the source wavelet. Elastic finite-difference models of the reflection data (J. M. Howie *et al.*, manuscript in preparation, 1992) that estimate the random scattering and reflective properties of the Transition Zone crust show no phase alteration of the propagating signal through the models. This observation implies that while the filtering effect by the Earth  $e(t)$  reduces the bandwidth of the data, it does not significantly alter the phase.

We employ the extracted source signature from the direct arrival to create synthetic seismograms with the reflectivity method of Fuchs [1968] and to deconvolve the data and synthetics for comparison purposes. The deconvolved events that are resolvable in the lower crust match best with deconvolved synthetic reflections generated from thin (less than 200 m thick), high-velocity layers of positive reflection polarity. As will be shown, this result is consistent with a comparison of  $P$  and  $S$  wave reflectivity and with the observed  $P$  wave reflection amplitude versus offset. Our findings are most consistent with laminated lower crustal events resulting from thin, high-velocity layers in the lower crust, probably horizontal magmatic intrusions.

#### CALIBRATION OF THE SOURCE WAVELET

Stanford University collected vertical incidence, deep crustal seismic data in 1987 as part of an earlier segment of the PACE program that focused on the boundary between the southern Transition Zone and Basin and Range Province [Goodwin *et al.*, 1989; Goodwin and McCarthy, 1990]. A high signal-to-noise ratio allowed Goodwin *et al.* [1989] to directly determine the polarity and thickness of the Bagdad events, and the same reflection sequence is tied to the 1989 Stanford spread by the COCORP Arizona profiles. The direct arrival from shot 32 (Figure 1) appears clean and is comparable to the source wavelet extracted by Goodwin *et al.* [1989] in similar recording conditions (Figure 4). If the Bagdad reflection (br) sequence is known to have a positive polarity, then we can establish the validity of the extracted source wavelet from shot 32 and test the deconvolution operation (Figure 5). The deconvolution is performed as a division of the Fourier transform of the data and extracted source wavelet and is scaled in the frequency domain and then transformed back to the time domain. A high-amplitude Bagdad event from shot 32 (Figure 3) was corrected for normal move-out and surface statics, and adjacent traces were stacked to improve the signal-to-noise ratio. The stack of the Bagdad event matches best with the high-velocity reflection synthetic generated with the extracted source wavelet and has a positive reflection polarity (Figure 5). The deconvolution of the Bagdad stack also matches closely with the deconvolution of the synthetic high-velocity reflection. This similarity of the deconvolved stack and the synthetic establishes that the direct arrival is a valid representation of

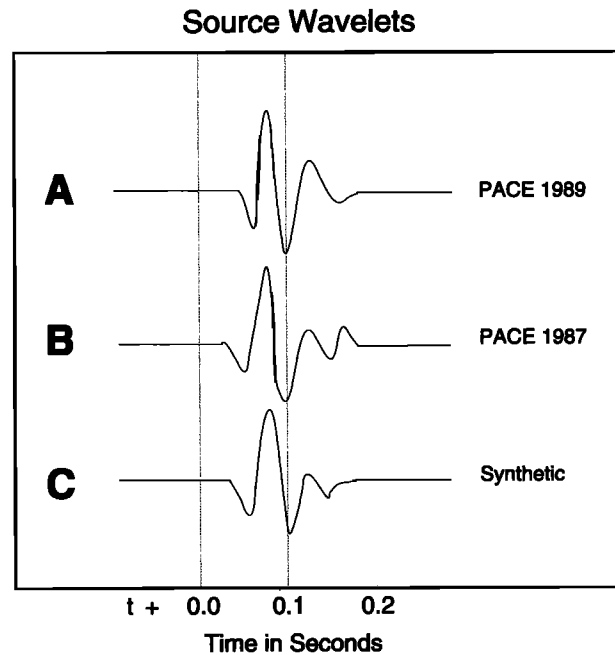


Fig. 4. (a) The extracted and tapered source wavelet used in this study. The wavelet was extracted from the direct arrival at 1.1 km offset and was recorded on granitic rocks. (b) The source wavelet from the Stanford 1987 Transition Zone experiment used by Goodwin *et al.* [1989] to find the reflection polarity of the Bagdad reflection sequence. (c) The wavelet generated by convolving a theoretical explosive source and ghost with recording array parameters [after Goodwin *et al.*, 1989].

the source character for both generation of synthetic reflections and source deconvolution. It is important to emphasize that the use of the term "deconvolution" in this case implies a simple spectral division of the wavelet from the data as opposed to the use of a seismic deconvolution processing package.

#### LOWER CRUSTAL REFLECTIONS

The near-vertical incidence data collected on the Stanford array during the PACE 1989 study are reflective beginning at about 6 s twt (Figure 2). At that depth (reflective zone spans approximately 19–27 km) the higher frequencies are attenuated and the frequency bandwidth narrows significantly (Figure 6). We model reflections as thin (100 m) layers (quarter wavelength  $\lambda/4$ ) and limit the frequency bandwidth used to generate the synthetics to be the same as that recorded from the lower crust (central frequency of approximately 16 Hz). The reflection waveform is not very sensitive to a particular layer thickness less than 200 m ( $\lambda/2$ ) because of the limited bandwidth. Reflection synthetics modeled with layers from 25 to 200 m thick are very similar in appearance, and such subtle differences are beyond the resolution of the lower crustal data.

The temporal resolution of the data is much reduced in the lower crust, and it is nearly impossible to discern a positive from a negative reflection polarity by inspection of the reflection. The waveforms of positive and negative reflection synthetics differ by the relative heights of the first and second pulses (Figure 7), but the difference is very slight and would be difficult to determine in the presence of noise. The

## Bagdad Reflection and Synthetics

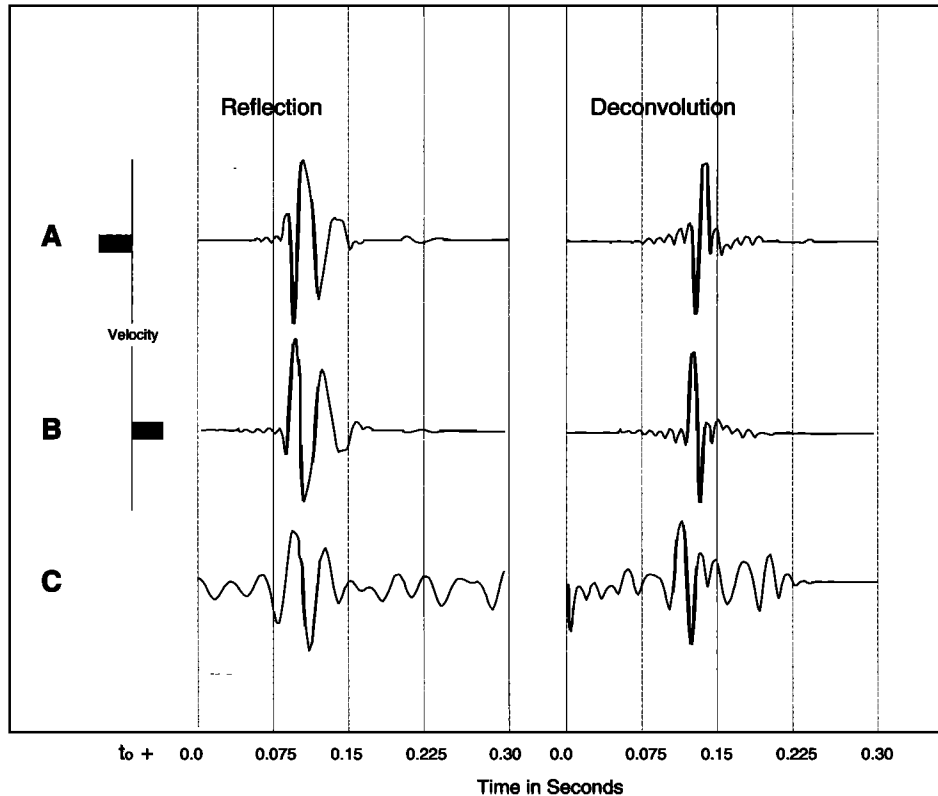


Fig. 5. (a) The synthetic reflection from a thin (25 m thick, approximately  $\lambda/8$ ), low-velocity layer (velocity contrast of 6.1 km/s to 5.4 km/s). The synthetic was generated with the reflectivity method of *Fuchs* [1968] using the extracted source wavelet shown as in Figure 4a. The source deconvolution resolves the reflection into an initially negative spike followed by a positive spike. (b) The synthetic reflection from a 25-m-thick, high-velocity layer (velocity contrast of 6.1 km/s to 6.8 km/s). The source deconvolution has an initial positive spike followed by a negative spike. (c) The stack of a Bagdad reflection event from 1.0 s two-way travel time (Figure 3, br 1). The Bagdad reflection stack most closely resembles the positive synthetic reflection and has a positive polarity. The source deconvolution has a positive followed by a negative spike, which also matches with the positive polarity synthetic. This result is consistent with the interpretation of the Bagdad events as thin, high-velocity layers and establishes the validity of the extracted source wavelet for use in reflectivity modeling and source deconvolution.

predicted amplitude of the initial lobes of the reflections is below noise levels, making the use of a convolutional forward modeling technique [e.g., *Pratt et al.*, 1991] impossible to apply. However, deconvolving the source wavelet from the synthetics resolves the reflections into a central peak of positive or negative polarity corresponding to the sign of the impedance used to generate the synthetics (Figure 7).

By windowing the reflective lower crustal portion of the data, we isolated clean reflections that are uncontaminated by other temporally close events (Figure 8). If events are too close together in time, the polarity is not decipherable because of interference; similarly, multicyclic events are difficult to resolve because they do not deconvolve into a single central peak. The cleanest lower crustal events were corrected for spherical divergence, static shifts, and normal move-out. Adjacent traces were then stacked along the central part of the reflection segments (approximately 0.3–1 km in horizontal extent) and deconvolved with the source wavelet. The deconvolutions of the cleanest lower crustal reflection stacks have a positive central peak and compare more closely to the deconvolution of the synthetic positive

reflection (Figure 7). To determine the validity of stacking events to find the reflection polarity, we deconvolved each trace of the reflections individually and found that the traces resolve to central positive peaks and that the stack of the deconvolved traces is nearly identical to the deconvolution of the stack (Figure 9).

The polarity determinations suggest that these lower crustal reflections probably result from positive impedance contrasts. The limited bandwidth and lower signal-to-noise ratio of the lower crustal reflections cause a degree of uncertainty in polarity determination, but the results are buoyed by the calibration with the Bagdad reflections in the upper crust and the close match with the synthetic modeling. *Meissner et al.* [1984] determined the polarity of a thrust-fault reflection beneath the Variscan front of northern Germany and found that the sheared zone of the fault plane is mostly low velocity but that the polarity tends to interchange along the reflection. Their observation is consistent with the Variscan front reflector consisting of a brecciated zone of mixed lithologies and changing pore pressure. The lower crustal reflections beneath the Colorado Plateau margin are of more consistent positive polarity, which leads us to

## Amplitude Spectra

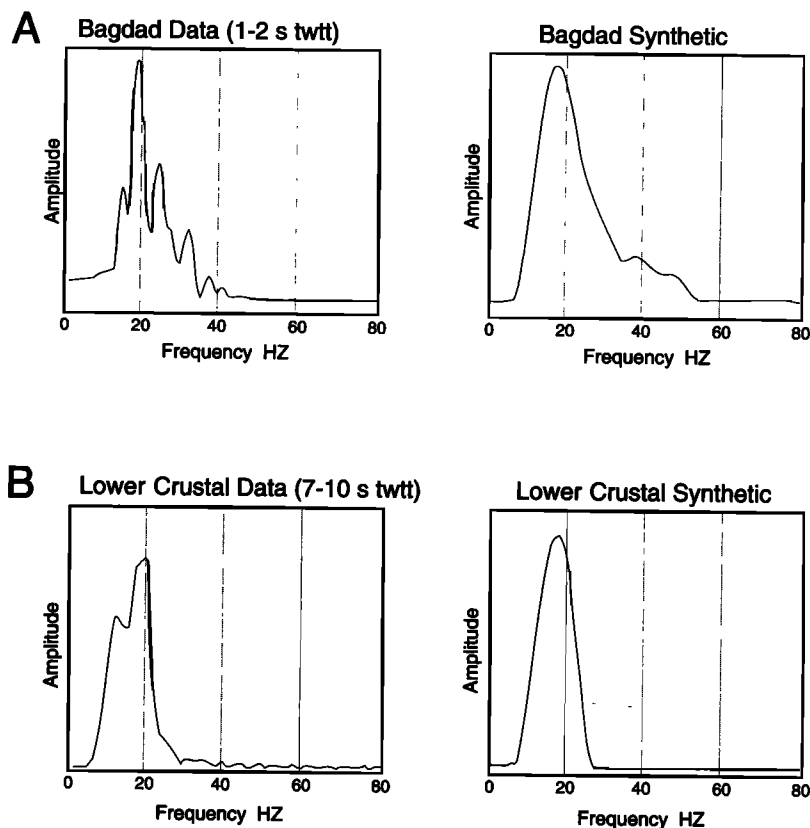


Fig. 6. Amplitude spectrum curves of the data and of the synthetic reflectivity models used in this study. (a) Amplitude spectrum of the Bagdad reflection events and of the synthetic Bagdad reflections. (b) Amplitude spectrum of the lower crustal reflectivity (from 7 to 10 s two-way-travel time (twtt)) and the spectrum of the synthetic lower crustal events. The reduced bandwidth of the lower crustal section results in much reduced temporal resolution, making the modeling of lower crustal events more difficult.

conclude that the reflectors are high-velocity lithologic contrasts rather than shear zones.

Because of the restricted frequency bandwidth, it is impossible to model the exact layer thicknesses causing the lower crustal reflections chosen for analysis. Synthetic modeling within the restricted bandwidth of the data predicts visible separation of reflections from the layer top and bottom if the layer thickness is between 200 and 250 m (Figure 10). However, it is extremely difficult to discern a reflection of a layer thinner than 200 m ( $\lambda/2$ ) thick from a simple velocity step on the field data, because the waveforms are too similar (Figure 10). The clean reflections that were deconvolved are simple and do not show any indication of separation between reflections from a layer's top and its bottom (Figures 7 and 8). Therefore the lower crustal reflections that were investigated for polarity are either (1) from layers 200-m ( $\lambda/2$ ) thick or less, (2) from layers much thicker than 200 m such that the reflection from the layer bottom is not near in time, or (3) from simple velocity steps. However, given that the reflections are of positive polarity, a series of strong positive velocity steps would raise the average velocity of the lower crust well beyond the maximum observed 6.5–6.6 km/s. Wide-angle reflections are not observed on the USGS PACE refraction data (J. McCarthy, personal communication, 1991) from the lower crust beneath the zone sampled by the Stanford spread as would be expected from

a series of high-velocity steps. Instead, we prefer to consider the reflections as resulting from high-velocity layers 200 m thick or less. It is likely that some of the more multicyclic events in the lower crust may be in the range from 200 to 250 m thick and that the reflection complexity is the result of separation of reflections from a layer top and bottom.

## P AND S WAVE RESPONSE

If laminated high-amplitude lower crustal reflectivity is due to shear zones, it is probably required either that such shear zones be fluid filled [Jones and Nur, 1982, 1984; Hyndman, 1988] or that the shearing juxtapose preexisting rock compositions and/or create thick mylonites [Christensen and Szymanski, 1988; Reston, 1990; Warner, 1990]. Partial melt and fluid-filled shear zones are expected to have a significantly increased *S* wave response relative to the *P* wave response [O'Connell and Budiansky, 1974; Moos and Zoback, 1983] because fluids lack shear rigidity and attenuate *S* waves more severely than *P* waves, which causes a large *S* wave velocity contrast across the layer boundary. Such a strong *S* wave impedance contrast causes a higher reflection coefficient for incident *S* waves than for *P* waves, while a lithologic contrast like a diabase intrusion or amphibolite layer has a smaller relative *S* wave impedance contrast [Goodwin et al., 1989; Jarchow, 1991]. The range of seismic

## Lower Crustal Reflections and Deconvolutions

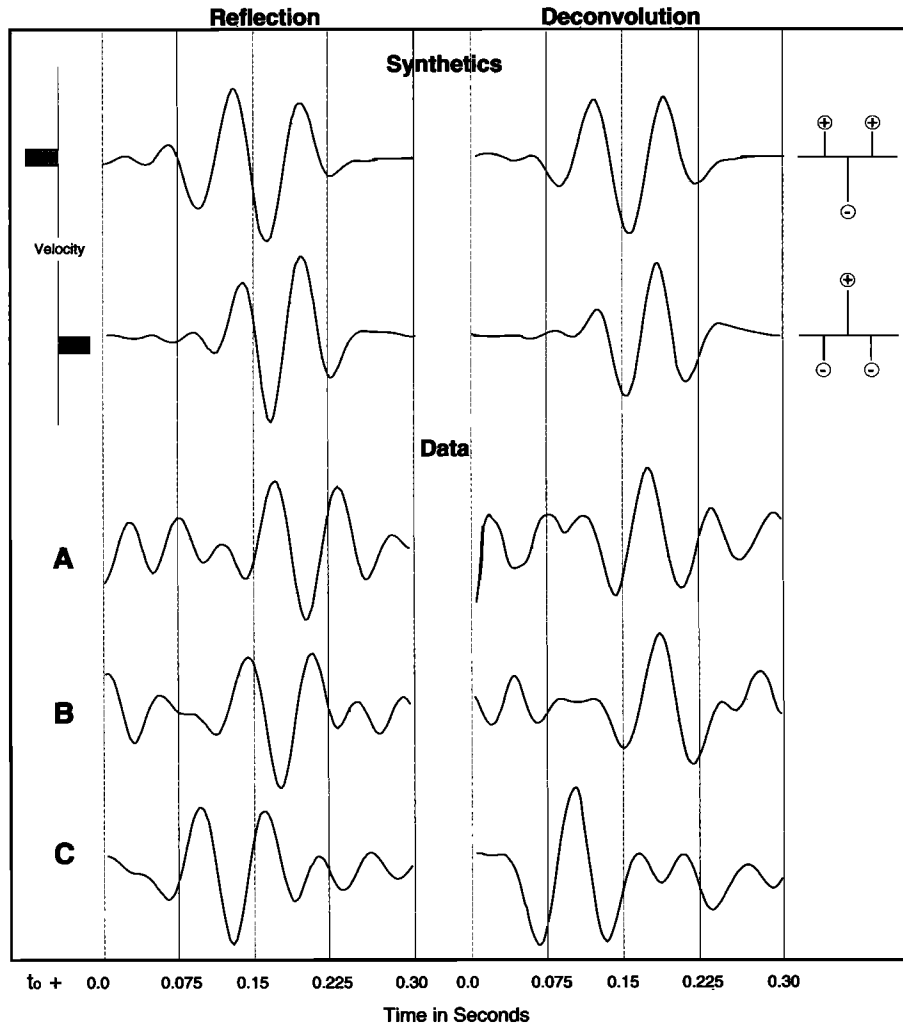


Fig. 7. Synthetic lower crustal reflections created with the restricted bandwidth of the lower crustal data utilizing the reflectivity method of *Fuchs* [1968]. The synthetic low-velocity reflection was generated with a contrast from 6.3 km/s to 5.7 km/s and a layer thickness of 100 m. The source deconvolution resolves to a negative central peak. The synthetic high-velocity reflection was generated with a contrast from 6.3 km/s to 6.9 km/s. The deconvolution of the high-velocity synthetic resolves to a positive central peak. The source deconvolutions of the synthetic lower crustal events are different in character from deconvolutions of the upper crustal Bagdad events because of the more limited frequency content of the lower crustal synthetics. The positive and negative polarity reflections look almost the same because of the limited spatial resolution and would be impossible to discern from each other in the presence of noise. Stacks of the cleanest lower crustal reflections (detailed in Figure 8) and corresponding source deconvolutions are shown in events A, B, and C. The deconvolutions most closely resemble the deconvolution of the positive synthetic reflection above and have positive central peaks, which implies that these lower crustal events result from high-impedance contrasts.

velocities and the densities of mafic intrusive rocks and mafic rocks of amphibolite grade are essentially identical [Kern and Richter, 1979; Christensen, 1982; Holbrook, 1988], making layers of magmatic intrusions seismically indistinguishable from metamorphic mafic layering. *S* waves are subject to greater attenuation and anisotropic effects than are *P* waves [e.g., Domenico and Danbom, 1987], and while it is difficult to quantify the exact amount of attenuation and anisotropic effect from the lower crust, some trends in relative *P* and *S* wave reflection amplitudes can be noted.

The comparison is valid on the Stanford data because of the presence of some bright *S* wave events near the base of lower crustal reflectivity, which shows that the *S* wave

energy has good depth penetration and is not overly attenuated (Figure 11). The background noise level on both the *P* and *S* wave sections is essentially identical because the data were collected over the same time window on the same recording system (apart from the use of horizontal geophones to record *S* waves). Thus any differences in the signal-to-noise ratio on the two sections is the result of differing signal. With the exception of the reflection at 16 s twtt on the *S* wave section (which corresponds to the reflection at 9.5 s twtt on the *P* wave section), the *S* wave section is generally less reflective than the *P* wave section corrected for spherical divergence (Figure 11). Reflections can be correlated from the *P* wave section to the *S* wave

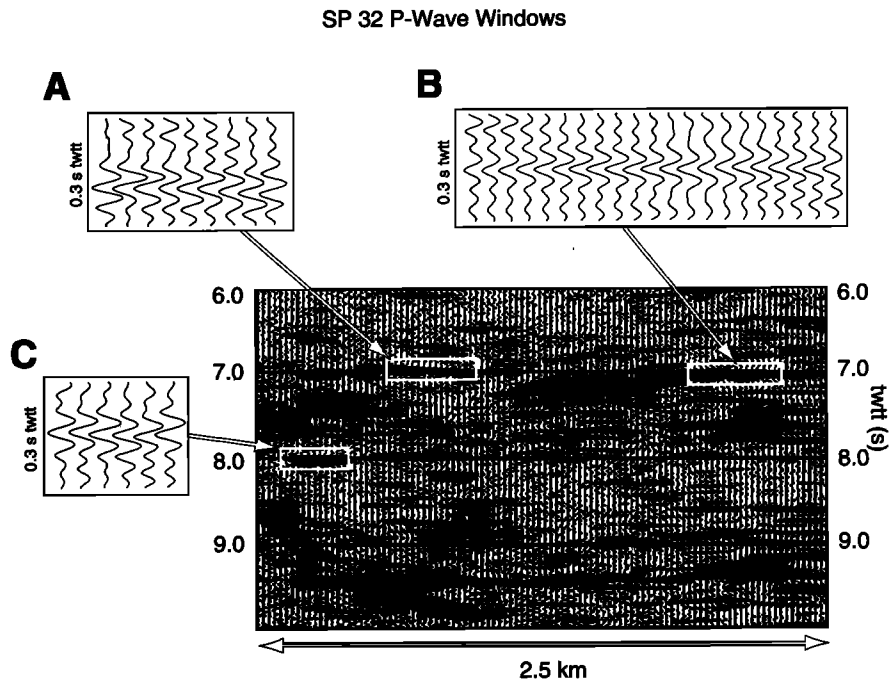


Fig. 8. Close-up windows of the reflective lower crustal zone beneath the Colorado Plateau margin. The reflections that are stacked and investigated for polarity are shown in detail. The reflections were chosen because they are isolated and uncontaminated by reflections too close above or below in time and are clean and simple in character.

section, but the *S* wave events are generally less continuous and are of lower apparent amplitude than are the *P* wave events. For example, the *P* wave reflection at 7 s twtt, which shows a positive reflection polarity upon deconvolution, is weak and discontinuous on the *S* wave section. *P* and *S* wave amplitude decay curves corrected for spherical divergence (Figure 11) confirm that the lower crust is generally more reflective to *P* waves than to *S* waves. While the *S* wave amplitude curve maintains a fairly constant trend from the near surface into the lower crust, the *P* wave amplitude

curve increases significantly with depth, particularly in the zone of lower crustal reflectivity. Examination of the 7-s *P* wave event which marks the top of the lower crust indicates that it is approximately 50% higher amplitude above the background than is the corresponding *S* wave reflection, which is consistent with a mafic reflector causing the events. In contrast with the bulk the lower crustal reflectivity, the 9.5 s twtt *P* wave event and the corresponding *S* wave reflection at 16 s twtt are of about the same amplitude (10 dB) above the background. This *S* wave event may in fact result

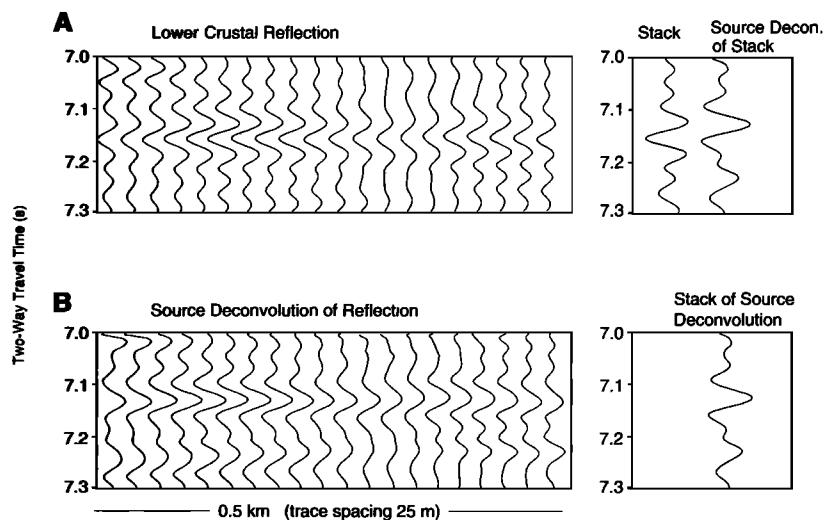


Fig. 9. (a) Close-up of lower crustal reflection (Figure 8 window B), the stack of the reflection, and the source deconvolution of the stack. The source deconvolution has a central positive peak which indicates that the reflection is the result of a high-impedance contrast. (b) Individual deconvolutions of reflection traces in Figure 9a. Each deconvolution has a consistent positive central peak. The stack of the deconvolutions closely resembles the deconvolution of the stack, which implies that the reflection stack did not degrade the waveform.

## High Velocity Synthetic Reflections

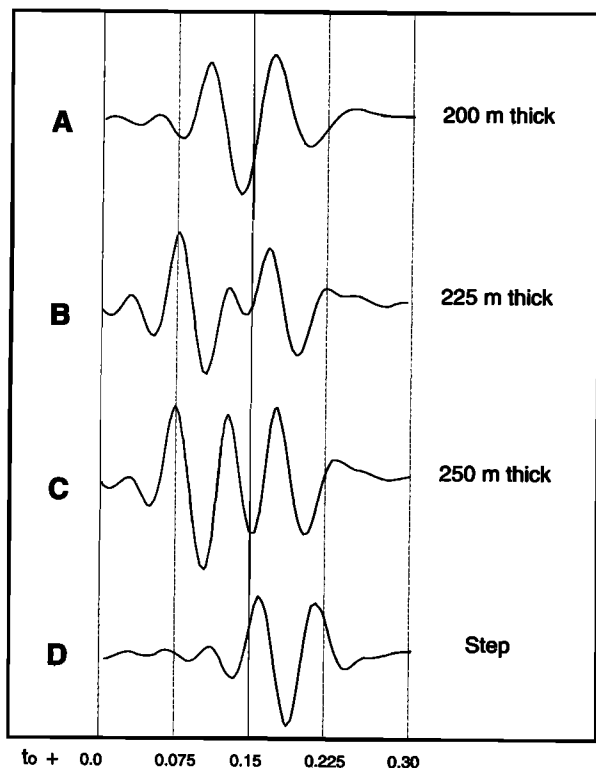


Fig. 10. Synthetic reflections from high-velocity layers (contrast from 6.3 km/s to 6.9 km/s) of increasing thickness. (a) The synthetic from a layer 200-m thick (approximately  $\lambda/2$ ), which is very similar to the synthetic of 100-m thickness in Figure 7. Because of the limited bandwidth, any layer 200 m thick or less will have a similar reflection character and be difficult to distinguish on field data. (b) The synthetic reflection from a layer of 225-m thickness. The reflection from the layer bottom begins to separate from the reflection off the layer top at this thickness. (c) The synthetic reflection from a 250-m-thick layer. At this thickness the reflection separation gives the event a multicyclic character, and layers of this thickness may be responsible for some of the multicyclic reflections observed in the lower crust beneath the Colorado Plateau margin. (d) The synthetic reflection from a simple velocity step. This reflection is again very similar to the reflection of Wave A and leaves open the possibility that the clean lower crustal reflections result either from layers thinner than 200 m thick or from layers thick enough to be essentially velocity steps. The low average velocity of the lower crust in this region [Kohler and McCarthy, 1990] and laminated appearance of the reflections cause us to model the events as thin layers.

from a higher reflection coefficient than the  $P$  wave coefficient, when the greater  $S$  wave attenuation is taken into consideration, which could indicate the presence of fluids. The  $P$  wave amplitude of the 9.5-s reflection at 10 dB is comparable to relative amplitudes reported for the Death Valley, Socorro, Surrency (8.5–10 dB) [Brown et al., 1987], and Buena Vista (17 dB) [Jarchow, 1991] bright spots. The Death Valley, Socorro, and Buena Vista bright spots are interpreted as magma bodies. The 9.5 s twtt  $P$  wave reflection is multicyclic, and attempts to deconvolve the reflection for polarity were not conclusive. Many compositional-layer models might be developed to satisfy the relative  $P$  and  $S$  wave amplitude observations, so we employ the comparison primarily as a means to confirm other independent observations.

 $P$  WAVE AMPLITUDE VERSUS OFFSET

In an attempt to further constrain the origins of the lower crustal reflectivity beneath the Colorado Plateau margin, we modeled the behavior of two simple end-member causes for lower crustal reflectivity with increasing shot-receiver offset: fluid-filled shear zones or partial melts, and mafic layers of intrusive or metamorphic origin. Because the Stanford array recorded large explosive sources spaced at 5- to 10-km intervals, a continuous range of shot-receiver offsets for the same midpoints was not available. A semicontinuous range of incidence angles from about  $10^\circ$  to  $40^\circ$  was recorded from four explosive sources; the midpoints from these four shots correspond to the zone investigated for polarity and  $P$  and  $S$  wave reflectivity. The shots were of different sizes and were fired in different surface rock types ranging from granite and limestone to unconsolidated alluvium (Figure 1). Without uniform sources, reliable determination of reflector composition was not possible; however, the predicted behavior of the two end-member models as a function of offset can be noted. The fluid model predicts a steady decrease of reflection amplitude toward zero at about a  $40^\circ$  angle of incidence, while the mafic layer model predicts that the reflection amplitudes will decline more gradually and will begin to increase between  $30^\circ$  and  $40^\circ$  of incidence angle (Figure 12). The models are a simulation of reflected  $P$  wave energy impinging on the top of the reflective lower crust at 7 s twtt, and the amplitude curves for thin layers are generated for a central frequency of 16 Hz with the reflectivity code of Fuchs [1968] and the extracted source signature employed previously in this paper for the polarity analysis. The velocities for the low-velocity model are based on a zone of fully saturated cracks [O'Connell and Budiansky, 1974] or at least 15% partial melt [Mavko, 1980; Sato et al., 1989; Jarchow, 1991], while the velocities for the high-velocity layer model correspond to a pressure-corrected diabase or amphibolite layer [Kern and Richter, 1979; Christensen, 1982; Holbrook, 1988]. We recognize that many possible models for lower crustal reflectors exist, but limitations in the offset range of the data force us to model end-member conditions.

Amplitude decay curves corrected for normal move-out show that the top of the lower crust is reflective throughout the offset range investigated, which is more consistent with the high-velocity mafic layer model than with the fluid-filled shear zone or partial melt model (Figure 13). While the absolute reflection amplitudes are perhaps not meaningful because of differing source conditions, the reflection event from the top of the lower crust is distinct on all the amplitude decay curves and stands out well above the noise level. The event is discernible on true amplitude data windows (Plate 1) and does not appear to fade with offset, as would be the case if the reflectors were fluid zones. In contrast, the reflection at 9.5 s twtt has high amplitude (10 dB) through  $13^\circ$  (corrected for greater depth) of incidence angle (shot point (SP) 32), but disappears at larger offsets of  $28^\circ$  (SP 62) and  $38^\circ$  (SP 56) of incidence angle (Figure 13, Plate 1). The abrupt reflection amplitude decrease of the 9.5-s event is consistent with the fluid model, as is the  $S$  wave response of the event. The indication from seismic modeling is that much of the lower crustal reflectivity is the result of high-velocity layers but that the 9.5-s event is of much different character and probably is the result of a fluid-saturated or partial melt zone.

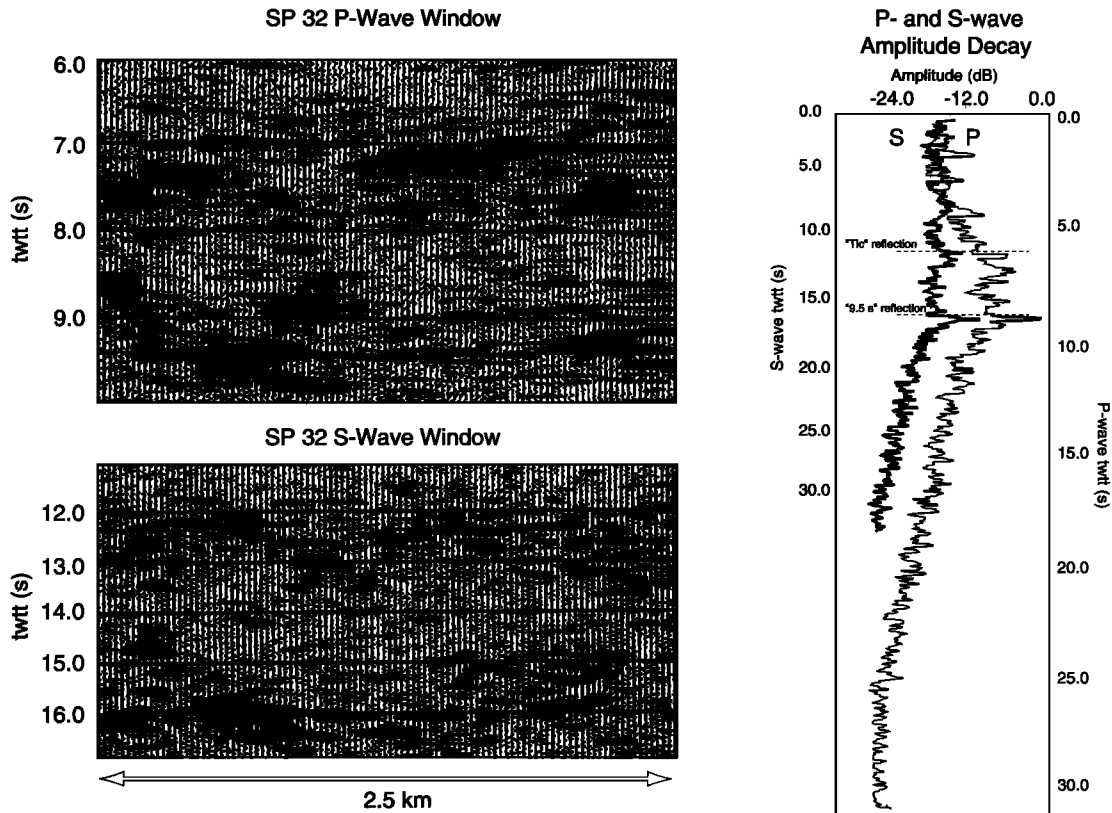


Fig. 11. *P* and *S* wave windows of the lower crustal reflectivity beneath the Colorado Plateau margin. The data were not corrected for normal move-out but were corrected for spherical divergence, and a band-pass filter was applied (16–35 Hz, *P* wave; 2–12 Hz, *S* wave). The *S* wave time scale was compressed assuming a Poisson's ratio of 0.25 to enable a direct comparison of reflection events from the *P* to *S* wave sections. The *S* wave reflections have in general lower amplitude than the *P* wave section, and the *S* wave events tend to be less horizontally continuous. Reduced *S* wave reflectivity might be attributed to greater seismic attenuation and anisotropy effects, but the *S* wave event at 16 s two-way travel time (twtt) is nearly equal in amplitude (10 dB with respect to the background) to the corresponding *P* wave event at 9.5 s twtt as shown by the amplitude decay curves, implying that there was good *S* wave energy penetration. We attribute the reduced *S* wave reflectivity primarily to lower relative *S* wave reflection impedance, such as high-velocity lithologic contrasts associated with horizontal diabase intrusions. The bright *S* wave event at 16 s twtt is nearly unique in this data set and probably results from a greater relative impedance contrast than the corresponding *P* wave reflection. A stronger *S* wave impedance contrast is a possible indication of the presence of fluids.

#### TECTONIC SIGNIFICANCE OF THIN, HIGH-VELOCITY LAYERING IN THE LOWER CRUST

The results of reflection polarity, *P* and *S* wave reflectivity, and *P* wave amplitude versus offset analyses are consistent with many lower crustal events beneath the Transition Zone of the Colorado Plateau reflecting from thin, high-velocity layering. The two most likely causes of high-velocity layers in the lower crust are horizontal diabase intrusions and mafic layers created by shearing and subhorizontal alignment and segregation of minerals during ductile flow [e.g., *Wever and Meissner, 1987; Green et al., 1990*]. The most reflective lower crustal zones recorded in the Transition Zone on the Stanford reflection profiles of 1987 [*Goodwin and McCarthy, 1990*] and 1989 correspond to the highest regional surface heat flow (Figure 14) (*J. Sass and A. Lachenbruch, unpublished data, 1991*). The lower crustal reflectivity fades laterally beneath the nonextended Colorado Plateau [*Howie et al., 1991; J. M. Howie et al., manuscript in preparation, 1992*], and surface heat flow values drop off correspondingly, although the observed surface heat flow on the Colorado Plateau may be complicated by upper crustal groundwater circulation. Active nor-

mal faults in the Transition Zone are widely spaced and have moderate displacements, indicating that extension has been minor ( $\approx 10\%$ ) compared with the neighboring, highly extended ( $\approx 35\text{--}100\%$ ) Basin and Range Province [*Zoback et al., 1981*]. In order for strain-induced lithologic layers or strongly mylonitic zones to be created, the crust must be subjected to an extreme degree of tectonic strain [e.g., *Warner, 1990*], probably much beyond the minor extension undergone in the Transition Zone. Conversely, in order for horizontal magmatic intrusions to be emplaced, the degree of extension need only be large enough for vertical magma conduits to form, which is possible even in weakly extended terranes.

The most commonly observed xenoliths in eruptive basalts of the Transition Zone are mafic igneous rocks that were originally intruded into a zone spanning 10 km above and below the Moho [*Wilshire, 1990*]. There has been a northeastward progression of late Cenozoic volcanic activity across the Transition Zone and into the Colorado Plateau [e.g., *McKee and Anderson, 1971; Armstrong and Ward, 1991*]. *Moyer and Nealey [1989]* summarize the trend of rhyolite eruptions across the Transition Zone, which become

## Predicted AVO Response Thin Layers (16 Hz Central Frequency)

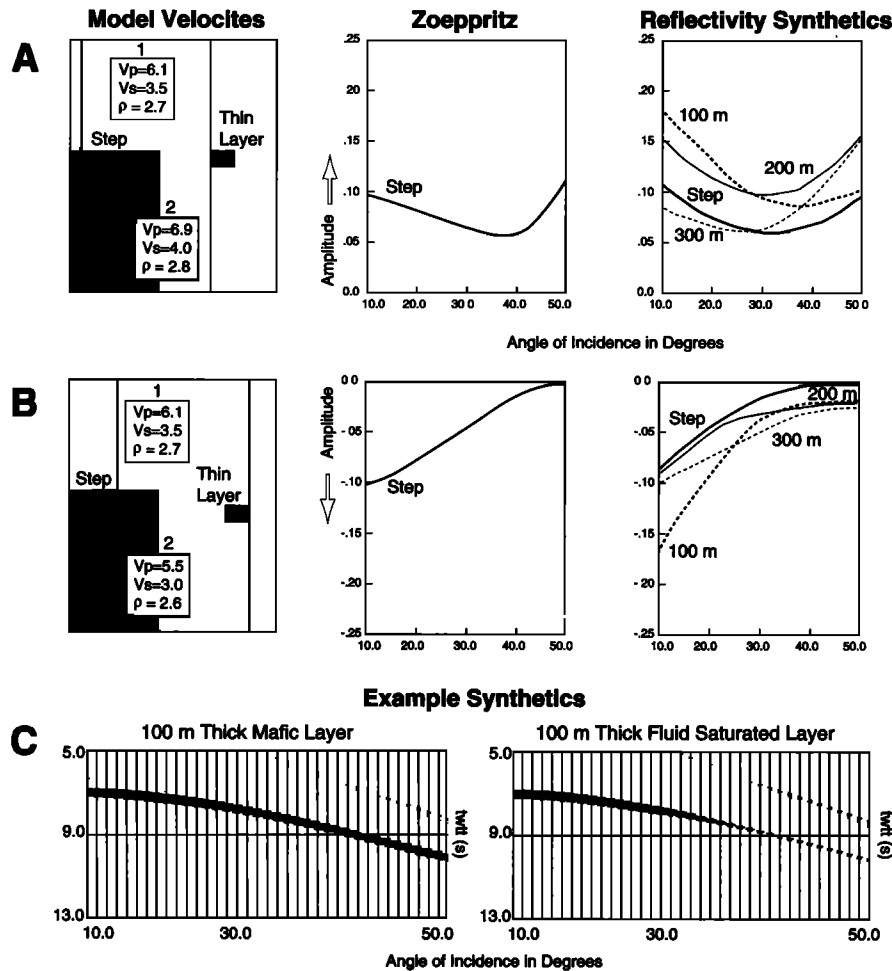


Fig. 12. Models of  $P$  wave amplitude versus offset (AVO) of two simple end-member causes of lower crustal reflectivity: high-velocity mafic layers and low-velocity fluid-filled shear zones or partial melts. Reflectivity synthetics [Fuchs, 1968] were used to predict the AVO trend of thin layers and a simple velocity step and were held to the same frequency range as the lower crustal data (16-Hz central frequency). The step response was also calculated using the Zoeppritz equations and compares well to the step model generated with the reflectivity method. (a) The mafic layer model predicts that the amplitude of reflections with increasing offset declines gradually to about  $30^{\circ}$ – $40^{\circ}$  of incidence angle, where it begins to increase. (b) The fluid-filled shear zone or partial melt model predicts a more pronounced reduction in amplitude with offset through about  $50^{\circ}$  of incidence angle. For example, a 100-m-thick mafic layer is predicted to have about twice the amplitude of a fluid-saturated layer at an offset of  $30^{\circ}$ . (c) Example synthetic record sections of the two end-member models showing the relatively consistent reflection amplitude with offset of a 100-m-thick mafic layer compared with the reduced reflection amplitude from a fluid-saturated layer. The low-amplitude part of the fluid-saturated layer reflection would probably be lost in the noise on field data.

progressively younger from a maximum of 15.1 Ma at the southern edge of the Transition Zone at the Casteneda Hills field to as young as 2.7 Ma at the Colorado Plateau margin in the Mount Floyd field. There is evidence for a northeastward younging progression within volcanic fields of the southern Colorado Plateau at the San Francisco field [Tanaka *et al.*, 1986] and at the Springerville field [Condit *et al.*, 1989] which has been attributed to southwestern motion of the North American plate relative to stationary plumes. Nealey and Sheridan [1989] show that the bulk of magmatic activity of the northern Transition Zone occurred from 10 to 5 Ma and that the activity has shifted northward into the Colorado Plateau during the past 5 m.y. Outcrops of basalt which are thought to be of Pliocene age are scattered across Chino Valley [Krieger, 1965]. Thus a northeast migrating pulse of

magmatism has passed through Chino Valley at the approximate rate of the North American plate and has probably been emplacing igneous rocks into the crust near the Colorado Plateau margin during the past 10 m.y.

While it is impossible from the seismic evidence to rule out compositional contrasts created by shearing in the lower crust or preexisting compositional layers as a cause for the observed reflectivity, the xenolith data and the late Tertiary pulse of magmatism in Chino Valley point toward at least some part of the reflectivity resulting from intruded igneous layers. The apparent presence of fluids near the base of the lower crustal reflectivity (the 16-s twtt  $S$  wave event) can be explained within the mafic intrusion model if the layer is a partially molten, recently emplaced magmatic intrusion. If igneous melts have been emplaced during the most recent

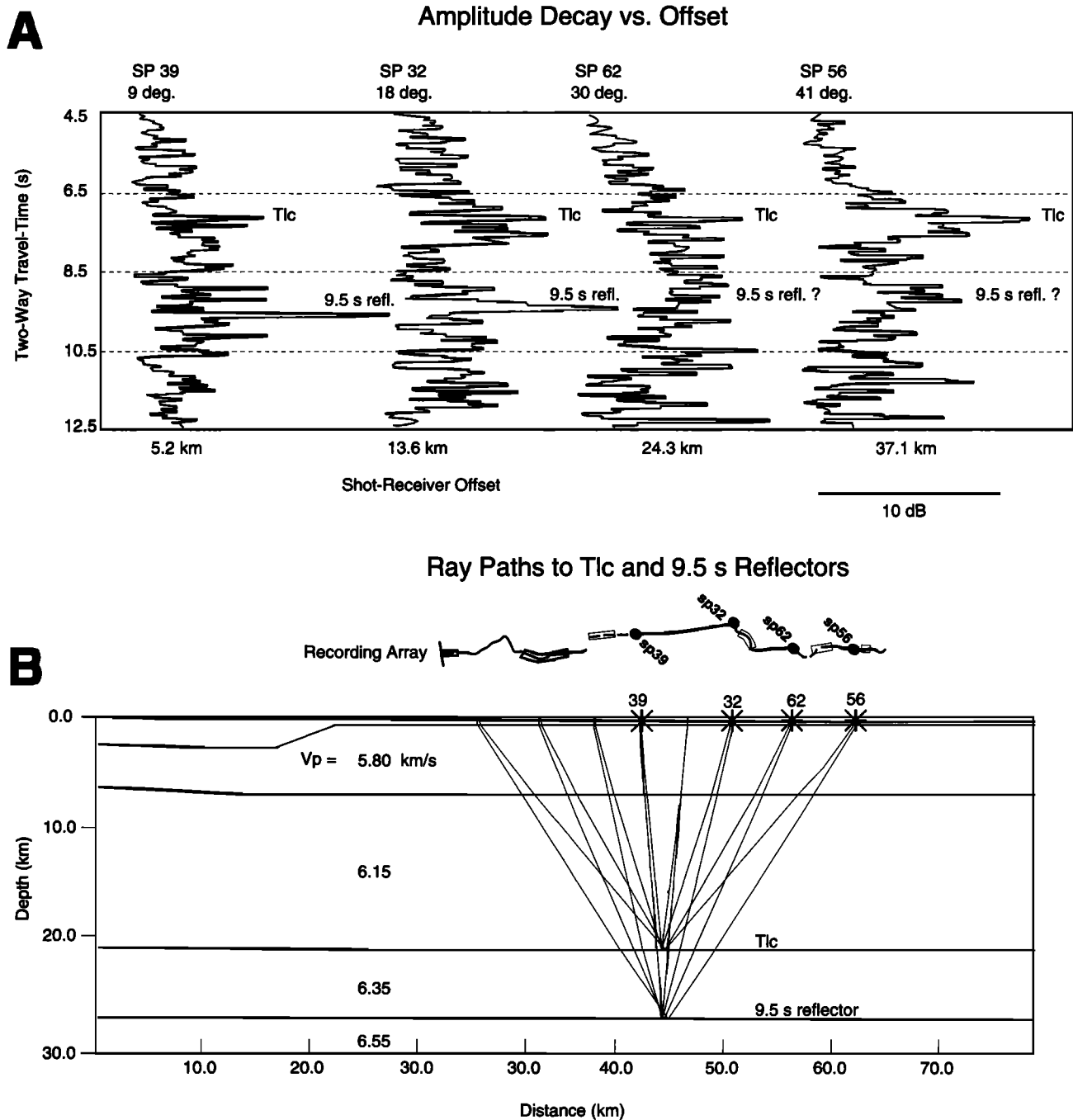


Fig. 13. (a) Amplitude decay curves from a stack of 20 traces of the same midpoints from four different shots of increasing shot-receiver offset. The top of the lower crust (Tlc) at about 7.0 s two-way travel time (twtt) is a distinct event on all four curves and corresponds approximately to one of the reflections investigated for polarity. The consistent amplitude of the Tlc event well above noise levels most closely matches the prediction of the mafic layer model. The 9.5-s twtt event that had a strong *S* wave response (Figure 11) is very high amplitude through about 13° (shot point (SP) 32) of incidence angle (incidence adjusted for depth) but disappears at greater offset. The *S* wave response and amplitude versus offset results point toward possible fluid involvement of the 9.5-s event, though neither method yields a completely unique solution. (b) Ray trace of reflection travel paths to the Tlc and 9.5-s reflections through a preliminary velocity model. The recording array geometry is plotted above at same horizontal scale to show the receiver locations. The boundaries are not as continuous as the model suggests, but were plotted across the model for simplicity. The rays bottom across about a 600-m zone on each interface. The amplitude envelope traces were stacked over a span of 1 km on the surface, and the true amplitude windows (Plate 1) include a zone 2.5 km wide, indicating that the disappearance of the 9.5-s reflection is not due to insufficient spatial sampling.

extension, they may be responsible for the observed high heat flow, which is a signature of active extensional terranes [Lachenbruch and Sass, 1978; Morgan and Golombek, 1984; Lachenbruch and Morgan, 1990]. If it is assumed that the

observed high heat flow had its genesis within the reflective lower crust, then the heat was generated at depths from 21 to 27 km and would be expected to arrive at the surface from approximately 6 to 10 m.y. after the thermal event [Lachen-

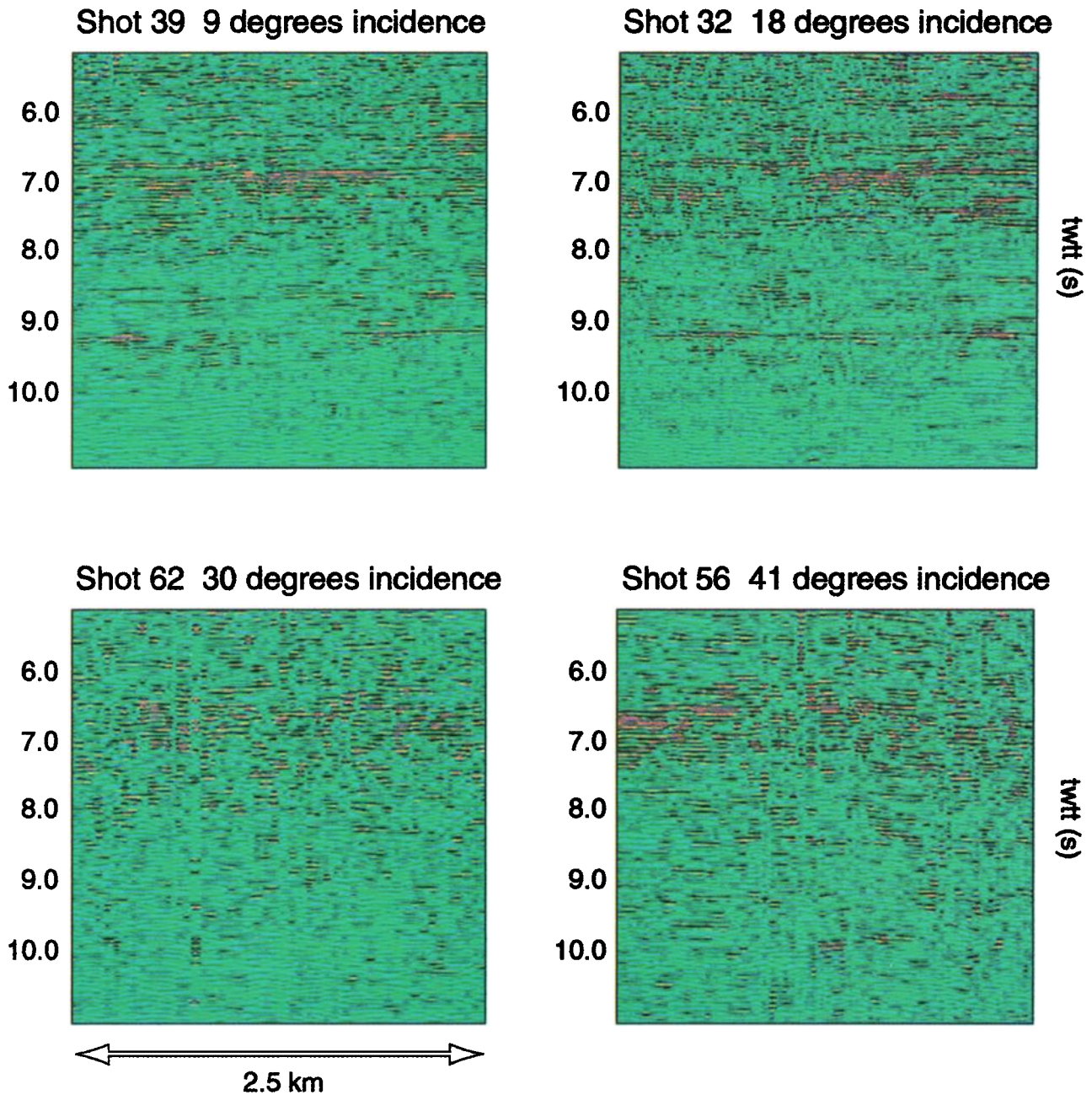


Plate 1. True-amplitude color contour images of the reflection sections at increasing offset; red corresponds to the highest positive amplitude and blue to the highest negative amplitude. The top of the lower crust is apparent on all the sections between 6 and 7 two-way travel time (twtt). The 9.5-s reflection is visible on shots 39 and 32 but is not evident at greater offset.

*bruch and Sass, 1978*]. Thus it is possible that the initial pulse of magmatism is represented in the observed heat flow, though it could also represent a broader mantle anomaly.

#### EMPLACEMENT OF HORIZONTAL INTRUSIONS AT A RHEOLOGICAL CONTRAST

The mechanism by which basaltic magma intrudes horizontally into extending crust is probably driven initially by the rapid intrusion of vertical dikes into the crust [*McCarthy and Thompson, 1988; Parsons and Thompson, 1991*]. The most common explanation for horizontal intrusions is melt ponding at a level of neutral buoyancy, the depth at which the melt and host rock are of equal density [*Bradley, 1965;*

*Herzberg et al., 1983; Corry, 1988; Baer and Reches, 1991*]. The difficulty with the ponding explanation is that it requires the melt to be able to penetrate the pores of the host rock or the host rock to behave as a fluid in order for the melt to interflow sufficiently to sense the host rock density. Both shallowly and deeply intruded mafic dikes tend to have chilled margins, implying that the melt is unable to penetrate the host rock pores, and over the rapid intrusion duration even ductile lower crustal rocks will act elastically [*Rubin, 1990*]. The horizontal intrusion process is more likely akin to the emplacement of vertical dikes, which is governed by the ambient stress field in the host rock which controls their orientation and thickness [*Anderson, 1951; Nakamura, 1977;*

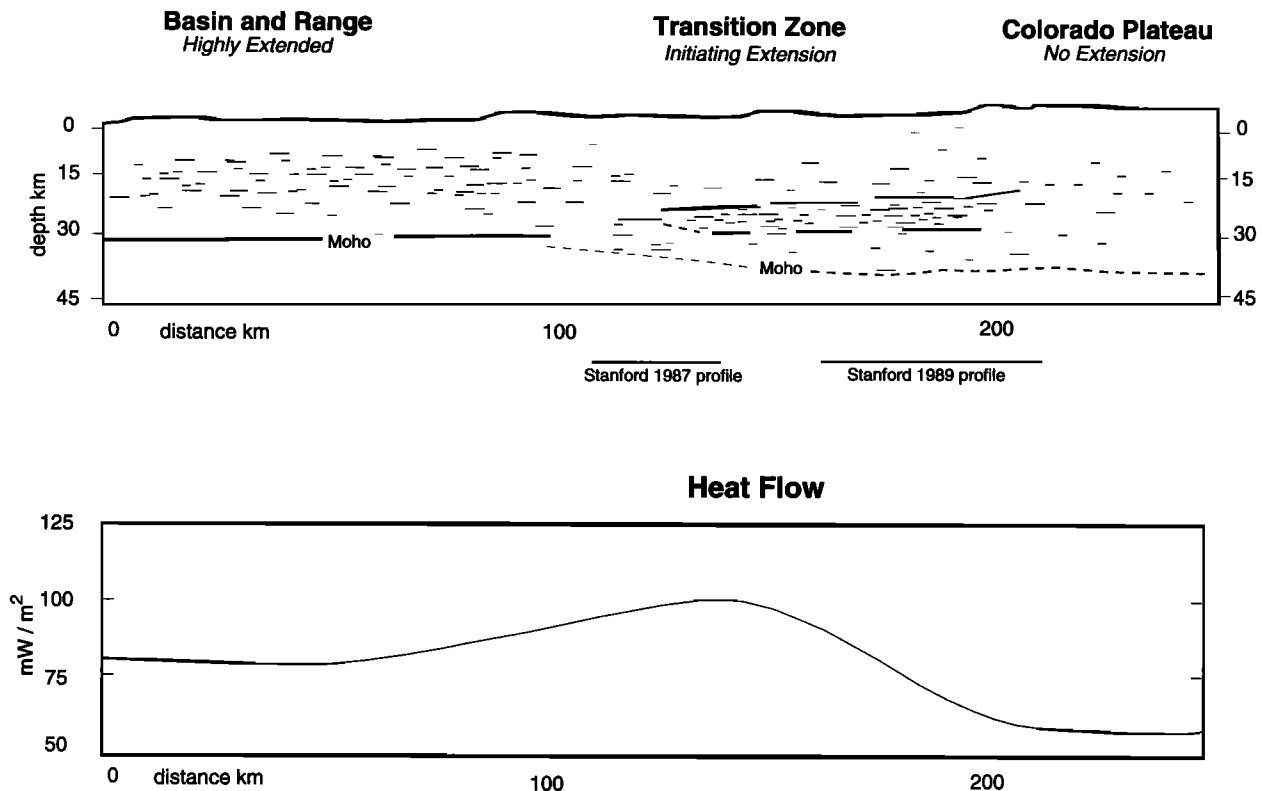


Fig. 14. Composite schematic plot of reflectivity inferred from the Stanford 1989 and 1987 reflection experiments in the Transition Zone, USGS PACE refraction data, and the COCORP Arizona profiles [Hauser *et al.*, 1987; Goodwin and McCarthy, 1990]. Heat flow is plotted below, as derived from the contour map of J. Sass and A. Lachenbruch, (unpublished data, 1992). There is a correlation between high heat flow, active seismicity, and lower crustal reflectivity in the Transition Zone.

Zoback and Zoback, 1980; Rubin and Pollard, 1988]. Vertical dikes intrude into extending terranes perpendicular to the horizontal least principal stress, whereas horizontal intrusions are favored when the least principal stress is vertical.

When vertical dikes intrude into extending crust, they are capable of accommodating much of the accumulated deviatoric stress in the host rock and are observed to supplant normal faulting in the brittle upper crust in regions where the magma supply is sufficient [Parsons and Thompson, 1991]. Vertical dikes push out against their walls in opposition to the least principal stress as they intrude, which increases the least stress. Multiple, rapidly intruding dikes are capable of overinflating the crust locally, creating a stress regime more favorable for the intrusion of horizontal sheets. The stress effect that dikes have on the host rock is magnified when they impinge on a rheologic boundary in the crust because zones of different rheology accumulate different levels of elastic stress [Parsons *et al.*, 1992]. For example, a dike crossing the crust-mantle boundary is likely to encounter smaller tectonic stress accumulations in the weaker, more ductile lower crust than it did in the stronger upper mantle. Thus the dike will cause a larger horizontal stress increase in the lower crust than in the upper mantle, and if more dikes follow, they may overinflate the lower crust, thereby initiating a horizontal intrusion at the crust-mantle boundary. Such a process would occur at any strong rheologic contrast within the crust.

Utilizing correlated *P* and *S* wave reflection events to get estimates of Poisson's ratio within the reflective lower crustal zone beneath the Colorado Plateau margin has con-

sistently yielded anomalously low values (0.15–0.25) for that depth in the crust (J. M. Howie *et al.*, manuscript in preparation, 1992). While the interpretation of Poisson's ratio is nonunique in terms of rock type, low Poisson's ratios are often associated with high quartz content [Tarkov and Vavakin, 1982], and quartz-rich rocks are rheologically weaker than rocks of more mafic composition [e.g., Smith and Bruhn, 1984; Kirby and Kronenberg, 1987]. Thus it is possible that basaltic melts have been trapped in a rheologically weak zone of lower deviatoric stress in the crust beneath the Transition Zone and have caused the horizontal intrusions seen as high-amplitude reflections in the lower crust. There is a general observation that laminated reflectivity is most often associated with rheologically weak zones [Meissner and Kuszniir, 1987; Wever and Meissner, 1987], and perhaps trapping of melts and subsequent horizontal intrusion within weak zones is in part the cause of laminated reflectivity. Goodwin and McCarthy [1990] and Ward and Warner [1991] observe a more constant increase with depth of Poisson's ratio with reported values from 0.27 to 0.30 for the lower crust. However, the lower crustal regions investigated by these workers are more densely reflective, and if a significant portion of the lower crust is intruded by mafic rocks, an increase in Poisson's ratio would be expected.

It is probable that some degree of shearing has occurred during ductile deformation in the lower crust beneath the Colorado Plateau margin. A significant amount of strain could have occurred if ductile lower crustal rocks flowed into the highly extended core complexes of the Basin and Range Province to the south when they were active through

the middle Miocene [McCarthy *et al.*, 1991]. However, the crustal thickness of the northern Transition Zone is essentially the same as the nonextended southern Colorado Plateau [Kohler and McCarthy, 1990; J. M. Howie *et al.*, manuscript in preparation, 1992; S. D. Ruppert, manuscript in preparation, 1992], implying that the amount of crustal flow from the Transition Zone has been minor. Thus while shearing and detachment zones have played an important role in the extreme extensional tectonics of the southern Basin and Range core complexes, the most recent tectonic picture of the Transition Zone is of mild extension encroaching into the Colorado Plateau, which is allowing occasional vertical intrusion and subsequent horizontal emplacement of magmatic sheets into the lower crust. Such magmatic sheets could account for the thin, high-velocity layers near the top of the lower crust as well as a deeper partial melt layer. The less continuous, multicyclic reflectivity observed on the section may be the result of compositional or metamorphic layering.

### CONCLUSIONS

1. Laminated lower crustal reflectivity observed from beneath the tectonically extended Transition Zone of the Colorado Plateau of central Arizona is similar in character to reflectivity observed in extended regions worldwide. The reflection polarity of the cleanest events from the lower crust appears positive, which suggests that these events result from thin (<200 m), high-velocity layering in the lower crust.

2. *P* and *S* wave reflectivity and *P* wave amplitude versus offset observations are more consistent with the investigated reflections resulting from mafic, high-velocity layers rather than fluid-filled shear zones or partial melts. One exception is a bright reflection at the base of lower crustal reflectivity which has a pronounced *S* wave response and demonstrates an abrupt decrease of *P* wave amplitude with offset, which is suggestive that the reflector may be a fluid-saturated shear zone or a partial melt.

3. The Transition Zone is a weakly extended province, and the magnitude of lower crustal shearing is expected to be minor compared with highly extended terranes. Because strain-induced juxtaposition of contrasting lithologies requires a significant degree of shearing, which is not supported by crustal thickness or geologic field mapping, we instead favor horizontal intrusion of basaltic magma as a mechanism to account for the thin, high-velocity layers. The most commonly observed xenoliths from the lower crust and upper mantle of the Transition Zone are of mafic igneous origin, which supports the suggestion that lower crustal reflectivity is the result of igneous intrusion. A pulse of magmatism crossed the Transition Zone into the Colorado Plateau during the late Tertiary period and was probably the source of intruded lower crustal mafic rocks.

4. Multiple, rapidly intruding overpressured dikes are capable of overinflating the crust locally, creating a stress regime more favorable for the intrusion of horizontal magmatic sheets. The imposed stress from dikes is magnified in rheologically weak zones because such zones develop less deviatoric stress, and subsequent magmatic intrusions are thus most likely to be trapped at rheological contrasts. The lower crustal reflectors of the Transition Zone reside in a zone of anomalously low Poisson's ratio, which could be an indication of weak, quartz-rich rheology. Magmatism may

have been concentrated in the weakest crust beneath the Transition Zone during the past 10 m.y. and would have contributed to the high observed heat flow.

*Acknowledgments.* Arco Oil and Gas Company and Amoco Production Company generously provided equipment and field support during the acquisition phase of the experiment. Jill McCarthy, Ed Criley, and Gray Jenson (USGS, Menlo Park) created a cooperative environment for university participants in the PACE program, and thanks are due to the USGS Deep Continental Studies Program for providing explosive sources. Processing and data analysis were possible because of computing and software resources generously made available by Jon Claerbout's Stanford Exploration Project and sponsors. This paper benefited immeasurably first from early reviews by Bruce Beaudoin, Simon Klemperer, and Jill McCarthy and later by Associate Editor Walter Mooney, Thomas Pratt, and one anonymous reviewer. The authors are grateful to Bruce Beaudoin, J. P. Blangy, Craig Jarchow, Stan Ruppert, and Norm Sleep for technical advice and support. We acknowledge financial support from the Gas Research Institute and NSF grants EAR 89-03541 and EAR 90-17667.

### REFERENCES

- Anderson, E. M., *The Dynamics of Faulting and Dyke Formation*, 206 pp., Oliver and Boyd, Edinburgh, 1951.
- Armstrong, R. L., and P. Ward, Evolving geographic patterns of Cenozoic magmatism in the North American cordillera: The temporal and spatial association of magmatism and metamorphic core complexes, *J. Geophys. Res.*, **96**, 13,201–13,224, 1991.
- Baer, G., and Z. Reches, Mechanics of emplacement and tectonic implications of the Ramon Dike Systems, Israel, *J. Geophys. Res.*, **96**, 11,895–11,910, 1991.
- BIRPS and ECORS, Deep seismic reflection profiling between England, France and Ireland, *J. Geol. Soc. London*, **143**, 45–52, 1986.
- Bradley, J., Intrusion of major dolerite sills, *Trans. R. Soc. N. Z. Geol.*, **3**, 27–55, 1965.
- Brown, L. D., *et al.*, COCORP: New perspectives on the deep crust, *Geophys. J. R. Astron. Soc.*, **89**, 47–54, 1987.
- Christensen, N. I., Seismic velocities, in *Handbook of Physical Properties of Rocks*, **2**, edited by R. S. Carmichael, pp. 1–228, CRC Press, Boca Raton, Fla., 1982.
- Christensen, N. I., Reflectivity and seismic properties of the deep continental crust, *J. Geophys. Res.*, **94**, 17,793–17,804, 1989.
- Christensen, N. I., and D. L. Szymanski, Origin of reflections from the Brevard fault zone, *J. Geophys. Res.*, **93**, 1087–1102, 1988.
- Clowes, R. M., E. R. Kanasevitch, and G. L. Cumming, Deep crustal seismic reflections at near-vertical incidence, *Geophysics*, **33**, 441–451, 1968.
- Condit, C. D., L. S. Crumpler, J. C. Aubele, and W. E. Elston, Patterns of volcanism along the southern margin of the Colorado Plateau: The Springerville field, *J. Geophys. Res.*, **94**, 7975–7986, 1989.
- Corry, C. E., Laccoliths; Mechanics of emplacement and growth, *Spec. Pap. Geol. Soc. Am.*, **220**, 110 pp., 1988.
- Domenico, S. N., and S. H. Danbom, Shear-wave technology in petroleum exploration—Past, current, and future, in *Shear-Wave Exploration*, edited by S. H. Danbom and S. N. Domenico, pp. 3–18, Society of Exploration Geologists, Tulsa, Okla., 1987.
- Eberhart-Phillips, D., R. M. Richardson, M. L. Sbar, and R. B. Herrman, Analysis of the 4 February 1976 Chino Valley, Arizona, earthquake, *Bull. Seismol. Soc. Am.*, **71**, 787–801, 1981.
- Fuchs, K., The reflection of spherical waves from transition zones with arbitrary depth-dependent elastic moduli and density, *J. Phys. Earth*, **16**, Special Issue, 27–56, 1968.
- Fuchs, K., On the properties of deep crustal reflectors, *J. Geophys.*, **35**, 133–149, 1969.
- Galvan, W. E., and E. G. Frost, Seismic reflection evaluation of detachment-related deformation in the transition zone, west-central Arizona (abstract), *Eos Trans. AGU*, **66**, 979, 1985.
- Goodwin, E., and J. McCarthy, The lower crust of the Transition Zone, Arizona, *J. Geophys. Res.*, **95**, 20,097–20,109, 1990.
- Goodwin, E., G. A. Thompson, and D. A. Okaya, Seismic identification of basement reflectors: The Bagdad reflection sequence in

- the Basin and Range Province—Colorado Plateau Transition Zone, Arizona, *Tectonics*, 8, 821–832, 1989.
- Green, A., et al., Origin of deep crustal reflections: Seismic profiling across high-grade metamorphic terranes in Canada, *Tectonophysics*, 173, 627–638, 1990.
- Hauser, E. C., J. Gephart, T. Latham, L. Brown, S. Kaufman, J. Oliver, and I. Lucchitta, COCORP Arizona Transect: Strong crustal reflections and offset Moho beneath the transition zone, *Geology*, 15, 1103–1106, 1987.
- Herzberg, C. T., W. F. Fyfe, and M. J. Carr, Density constraints on the formation of the continental Moho and crust, *Contrib. Mineral. Petrol.*, 84, 1–5, 1983.
- Hill, D. P., Phase shift and pulse distortion in body waves due to internal caustics, *Bull. Seismol. Soc. Am.*, 64, 1733–1742, 1974.
- Holbrook, W. S., Wide-angle seismic studies of crustal structure and composition in Nevada, California, and southwest Germany, Ph.D. thesis, 214 pp., Stanford Univ., Stanford, Calif., 1988.
- Howard, K. A., Intrusion of horizontal dikes: Tectonic significance of middle Proterozoic diabase sheets widespread in the upper crust of the southwestern United States, *J. Geophys. Res.*, 96, 12,461–12,478, 1991.
- Howe, J. M., T. Parsons, and G. A. Thompson, High-resolution P- and S-wave deep crustal imaging across the edge of the Colorado Plateau, USA: Increased reflectivity caused by initiating extension, in *Continental Lithosphere: Deep Seismic Reflections*, *Geodyn. Ser.*, vol. 22, edited by R. Meissner et al., pp. 21–29, AGU, Washington, D. C., 1991.
- Hyndman, R. D., Dipping seismic reflectors, electrically conductive zones, and trapped water in the crust over a subducting plate, *J. Geophys. Res.*, 93, 13,391–13,405, 1988.
- Jarchow, C. M., Investigations of magmatic underplating beneath the northwestern Basin and Range Province, Nevada, seismic data acquisition and tectonic problems of the Columbia Plateau, Washington, and the nature of the Mohorovičić discontinuity worldwide, Ph.D. thesis, 258 pp., Stanford Univ., Stanford, Calif., 1991.
- Jones, T. D., and A. Nur, Seismic velocity and anisotropy in mylonites and the reflectivity of deep crustal fault zones, *Geology*, 10, 260–263, 1982.
- Jones, T. D., and A. Nur, The nature of seismic reflections from deep crustal fault zones, *J. Geophys. Res.*, 89, 3153–3171, 1984.
- Kern, H., and A. Richter, Compressional and shear wave velocities at high temperature and confining pressure in basalts from the Faeroe Islands, *Tectonophysics*, 54, 231–252, 1979.
- Kirby, S. I., and A. K. Kronenberg, Rheology of the lithosphere: Selected topics, *Rev. Geophys.*, 25, 1219–1244, 1987.
- Klemperer, S. L., Deep seismic reflection profiling and the growth of the continental crust, *Tectonophysics*, 161, 233–244, 1989.
- Kohler, W., and J. McCarthy, PACE seismic refraction and wide-angle reflection studies of the Colorado Plateau—Basin and Range transition, Arizona (abstract), *Eos Trans. AGU*, 71, 1593, 1990.
- Krieger, M. H., Geology of the Prescott and Paulden quadrangles, Arizona, *U.S. Geol. Surv. Prof. Pap.*, 467, 127 pp., 1965.
- Lachenbruch, A. H., and P. Morgan, Continental extension, magmatism, and elevation; Formal relations and rules of thumb, *Tectonophysics*, 174, 39–62, 1990.
- Lachenbruch, A. H., and J. H. Sass, Models of an extending lithosphere and heat flow in the Basin and Range Province, in *Cenozoic Tectonics and Regional Geophysics of the Western Cordillera*, edited by R. B. Smith and G. P. Eaton, *Mem. Geol. Soc. Am.*, 152, 209–250, 1978.
- Levander, A. R., and B. S. Gibson, Wide-angle seismic reflections from two-dimensional random target zones, *J. Geophys. Res.*, 96, 10,251–10,260, 1991.
- Litak, R. K., R. H. Marchant, L. D. Brown, O. A. Pfiffner, and E. C. Hauser, Correlating crustal reflections with geological outcrops: Seismic modeling results from the southwestern USA and the Swiss Alps, in *Continental Lithosphere: Deep Seismic Reflections*, *Geodyn. Ser.*, vol. 22, edited by R. Meissner et al., pp. 299–305, AGU, Washington, D. C., 1991.
- Mavko, G. M., Velocity and attenuation in partially molten rocks, *J. Geophys. Res.*, 85, 5173–5189, 1980.
- McCarthy, J., and G. A. Thompson, The seismically reflective crust beneath highly extended terranes: Evidence for its origin in extension, *Geol. Soc. Am. Bull.*, 100, 1361–1374, 1988.
- McCarthy, J., S. P. Larkin, G. S. Fuis, R. W. Simpson, and K. A. Howard, Anatomy of a metamorphic core complex: Seismic refraction/wide-angle reflection profiling in southeastern California and western Arizona, *J. Geophys. Res.*, 96, 12,259–12,291, 1991.
- McKee, E. H., and C. A. Anderson, Age and chemistry of Tertiary volcanic rocks in north-central Arizona and relation of the rocks to Colorado Plateaus, *Geol. Soc. Am. Bull.*, 82, 2767–2782, 1971.
- Meissner, R., The “Moho” as a transition zone, *Geophys. Surv.*, 1, 195–216, 1973.
- Meissner, R., and N. J. Kusznir, Crustal viscosity and the reflectivity of the lower crust, *Ann. Geophys. Ser. B*, 5, 365–374, 1987.
- Meissner, R., and T. Wever, Nature and development of the crust according to deep reflection data from the German Variscides, in *Reflection Seismology: A Global Perspective*, *Geodyn. Ser.*, vol. 13, edited by M. Barazangi and L. Brown, pp. 31–42, AGU, Washington, D. C., 1986.
- Meissner, R., M. Springer, and E. Flüh, Tectonics of the Variscides in north-western Germany based on seismic reflection measurements, *Spec. Publ. Geol. Soc. London*, 14, 23–32, 1984.
- Moos, D., and M. D. Zoback, In situ studies of velocity in fractured crystalline rocks, *J. Geophys. Res.*, 88, 2345–2358, 1983.
- Morgan, P., and M. P. Golombek, Factors controlling the phases and styles of extension in the northern Rio Grande Rift, *Field Conf. Guideb. N. M. Geol. Soc.*, 35, 13–19, 1984.
- Moyer, T. C., and L. D. Nealey, Regional compositional variations of late Tertiary bimodal rhyolite lavas across the Basin and Range/Colorado Plateau boundary in western Arizona, *J. Geophys. Res.*, 94, 7799–7816, 1989.
- Nakamura, K., Volcanoes as possible stress indicators of tectonic stress orientation—Principle and proposal, *J. Volcanol. Geotherm. Res.*, 2, 1–16, 1977.
- Nealey, L. D., and M. F. Sheridan, Post-Laramide volcanic rocks of Arizona and northern Sonora, Mexico, and their inclusions, in *Geologic Evolution of Arizona*, edited by J. P. Jenney and S. J. Reynolds, *Ariz. Geol. Soc. Dig.*, 17, 609–647, 1989.
- O’Connell, R. J., and B. Budiansky, Seismic velocities in dry and saturated cracked solids, *J. Geophys. Res.*, 79, 5412–5426, 1974.
- Parsons, T., and G. A. Thompson, The role of magma overpressure in suppressing earthquakes and topography: World-wide examples, *Science*, 253, 1399–1402, 1991.
- Parsons, T., N. H. Sleep, and G. A. Thompson, Host rock rheology controls on the emplacement of tabular intrusions: Implications for underplating of extending crust, *Tectonics*, in press, 1992.
- Potter, C. J., C.-S. Liu, J. Huang, L. Zheng, T. A. Hauge, E. C. Hauser, R. W. Allmendinger, J. E. Oliver, S. Kaufman, and L. Brown, Crustal structure of north-central Nevada: Results from COCORP deep seismic profiling, *Geol. Soc. Am. Bull.*, 98, 330–337, 1987.
- Pratt, T. L., E. C. Hauser, T. M. Hearn, and T. J. Reston, Reflection polarity of the midcrustal Surrency Bright Spot beneath southeastern Georgia: Testing the fluid hypothesis, *J. Geophys. Res.*, 96, 10,145–10,158, 1991.
- Reston, T. J., Shear in the lower crust during extension: Not so pure and simple, *Tectonophysics*, 173, 175–183, 1990.
- Rubin, A. M., A comparison of rift-zone tectonics in Iceland and Hawaii, *Bull. Volcanol.*, 52, 302–319, 1990.
- Rubin, A. M., and D. D. Pollard, Dike-induced faulting in rift zones of Iceland and Afar, *Geology*, 16, 413–417, 1988.
- Sato, H., I. S. Sacks, and T. Murase, The use of laboratory velocity data for estimating temperature and partial melt fraction in the low-velocity zone: Comparison with heat flow and electrical conductivity studies, *J. Geophys. Res.*, 94, 5689–5704, 1989.
- Smith, R. B., and R. B. Bruhn, Intraplate extensional tectonics of the eastern Basin-Range: Inferences on structural style from seismic reflection data, regional tectonics, and thermal-mechanical models of brittle-ductile deformation, *J. Geophys. Res.*, 89, 5733–5762, 1984.
- Tanaka, K. L., E. M. Shoemaker, G. E. Ulrich, and E. W. Wolfe, Migration of volcanism in the San Francisco volcanic field, Arizona, *Geol. Soc. Am. Bull.*, 97, 129–141, 1986.
- Tarkov, A. P., and V. V. Vavakin, Poisson’s ratio behavior in various crystalline rocks: Applications to the study of the Earth’s interior, *Phys. Earth Planet. Inter.*, 29, 24–29, 1982.
- Ward, G., and M. Warner, Lower crustal lithology from shear wave reflection data, in *Continental Lithosphere: Deep Seismic Reflec-*

- tions, *Geodyn. Ser.*, vol. 22, edited by R. Meissner et al., pp. 343-349, AGU, Washington, D. C., 1991.
- Warner, M., Basalts, water, or shear zones in the lower continental crust?, *Tectonophysics*, 173, 163-174, 1990.
- Wever, T., and R. Meissner, About the nature of reflections from the lower crust, *Ann. Geophys. Ser. B*, 5, 349-352, 1987.
- Wilshire, H. G., Lithology and evolution of the crust-mantle boundary region in the southwestern Basin and Range Province, *J. Geophys. Res.*, 95, 649-665, 1990.
- Zoback, M. L., and M. D. Zoback, State of stress in the coterminous United States, *J. Geophys. Res.*, 85, 6113-6156, 1980.
- Zoback, M. L., R. E. Anderson, and G. A. Thompson, Cainozoic evolution of the state of stress and style of tectonism of the Basin and Range Province of the western United States, *Philos. Trans. R. Soc. London, Ser. A*, 300, 407-434, 1981.
- 
- J. Howie, T. Parsons, and G. Thompson, Department of Geophysics, School of Earth Science, Stanford University, Stanford, CA 94305-2215.

(Received November 18, 1991;  
revised April 15, 1992;  
accepted April 20, 1992.)